2012 NDIA GROUND VEHICLE SYSTEMS ENGINEERING AND TECHNOLOGY SYMPOSIUM
POWER AND MOBILITY (P&M) MINI-SYMPOSIUM
AUGUST 14-16, MICHIGAN

POWERTRAIN EMBEDDED DIAGNOSTIC AND PREDICTIVE CAPABILITY FOR AN AUTOMOTIVE TRANSMISSION

Mitchell Lebold,
Scott Pflumm, Jason Hines,
Jeffrey Banks,
and Jonathan Bednar
Applied Research Laboratory
The Pennsylvania State University
State College, PA 16804-0030
Telephone: (814) 865-8958
msl115@psu.edu

Larry Marino & Jim Bechtel
PM Heavy Brigade Combat Team
6501 E. 11 Mile Rd.
Warren MI, 48397

ABSTRACT

This report documents the investigation of a vibration-based diagnostic approach developed for automotive transmissions. Data was recorded throughout three durability tests that were conducted by the transmission OEM. Rebuilt transmissions were operated around the clock under the most demanding speed and load set-points until critical gear or bearing failures resulted in loss of operability.

The analysis results indicate that an embedded diagnostic and predictive capability can be implemented for military ground vehicle transmissions using vibration-based techniques. The results also specifically show an early indication of a fault condition is possible three weeks before failure for the test transmission. A technique for detecting solenoid faults using only the existing control signals rather than response measurements comparison that does not require the installation of additional sensors was also developed through this effort and will be discussed.

This paper highlights the diagnostics techniques for the bearing and solenoid faults. On-platform testing is suggested for technique validation and future development of these initial findings.

INTRODUCTION

Transmission Analysis Approaches - Statistical Analysis: Three statistical based analytical techniques were employed to enable fault detection and a predictive capability: Kurtosis, Crest Factor and a third technique collectively referred to as Combined Data Feature (CDF). Statistical approaches provide two main advantages for fault detection. The foremost advantage is the inherent capability to normalize and compare large and diverse set-point operating condition datasets. Second, statistical analysis improves the end user's ability to distinguish anomalies in the data. Some anomalies are indicative of machine degradation and the objective is to identify these anomalies as indications of impending failure. Other anomalies in the data obscure trends and require proper pre-processing treatment so as not to incorrectly interpret the data. Given that mechanical faults typically progress over time before resulting in failure, the statistical techniques below were selected because of their ability to detect and quantify these changes in the data over time.

DATA ANALYSIS ALGORITHMS

KURTOSIS

Kurtosis is the fourth statistical moment about the distribution mean, and can be computed from any signal or population distribution. In more general terms, kurtosis describes the relative length of the distribution tails. It provides a sensitive response to isolated impacts that are characteristic of many mechanical failures, which result in the distribution of the vibration data having thinner, and more elongated tails, and results in a higher kurtosis value. As a gear or bearing wears this feature should react to the increased level of vibration [1, 2, 3]. The equation for kurtosis is given by:

$$k = \frac{\Sigma_{n=1}^{N}[y(n)-\mu]^4}{N*(\sigma^2)^2}$$

where y(n) is the raw time series at point n, μ is the mean of the data, σ^2 is the variance of the data, and N is the total number of data points. A normal distribution has a kurtosis (K) value of 3.

VARIANCE

Variance is the measure of a sample's variability. The bias corrected sample variance is defined as

$$Variance \stackrel{def}{=} s_{N-1}^2 = \frac{1}{N}\sum_{i=1}^{N}(x_i-\mu)^2$$

Where N is the sample population and μ is the sample population mean. The square root of the variance is known as the standard deviation.

CREST FACTOR

The simplest approach to measuring defects in the time domain is using the RMS of the vibration. However, the RMS level may not show appreciable changes in the early stages of gear and bearing damage. Likewise, RMS can be affected by adjacent machinery vibration or in the case of mobile assets RMS may be affected by operating conditions (engine speed, and transmission range) and terrain roughness. RMS vibration levels also tend to differ between similar vehicles, due to a variety of differences in assembly, lubrication, and part wear. Changes in RMS vibration levels are affected by too many factors that are unrelated to mechanical condition. As a result, the use of RMS would lead to a high rate of false-detections.

A better measure is "crest factor" which is defined as the ratio of the peak level of the input signal to the RMS level. Therefore, peaks in the time series signal will result in an increase in the crest factor value.

For normal operations, crest factor may reach between 2 and 6. A value above 6 is usually associated with machinery problems. This feature is used to detect changes in the signal pattern due to impulsive vibration sources such as tooth breakage on a gear or a bearing defect pulsation. The crest factor feature is not considered a very sensitive technique. Below is the equation for the crest factor:

$$Crest\ Factor = \frac{PeakLevel}{RMS}$$

where *PeakLevel* is the peak level of the raw time series, and *RMS* is the root mean square of the raw data.

DATA FUSION

Data fusion is a technique used to combine quantities from multiple sources (sensor or feature based) to improve the inference ability over that of any individual indicator. An ideal diagnostic indicator would provide a highly correlated response to increasing damage, with higher values corresponding to increasing levels of damage. Individual statistical features that are commonly used for vibration-based diagnostics and prognostics do not always provide this ideal behavior. In some instances, the condition indicator will respond at early stages of damage initiation, and provide a sensitive diagnostic indicator. These types of features often do not provide a response that can be easily correlated to damage. Other condition indicators will lack the sensitivity to initiating damage, but respond in a manner that can be correlated to increasing levels of damage. Taking condition indicators of each type and fusing their responses together, can provide an individual damage sensitive feature that can be more easily interpreted in either a manual or automated fashion. Within this effort, several feature fusion techniques were investigated to improve the overall health related indicator.

As an initial investigation, common statistical features such as RMS, Variance, Kurtosis, and Crest Factor, were fused together to achieve a superior indicator than either of the features by themselves.

SOLENOID FAULT DETECTION APPROACH

Solenoids within the transmission are a single point of failure item which can render the transmission degraded or disabled. While these devices are replaceable in the field, currently there is no indication provided to the soldier to aid in troubleshooting. With a small embedded device to perform comparison logic, indication of range solenoid failure can be easily provided to the soldier.

The transmission's operational range (1st, 2nd or 3rd) is controlled by three solenoid operated valves. These valves control hydraulic pressure within the transmission internals for shifts between ranges. Each solenoid receives a binary

(high or low) command signal. The ARL's data acquisition system recorded the solenoid command signals as well as the 1st-3rd range pressure signals. By comparing the command signal to the resulting pressure signal, solenoid fault detection can be automated.

Table 1 summarizes the solenoid input, or command signal-operational range logic relationship. As shown, range #1 is engaged when command signal #1 is HIGH and command signals #2 and #3 are LOW. Range #2 actuation is similar to range #1. Range #3 solenoid is a special case and is actuated with negated logic.

	Operational Range		
	1st Range	**2nd Range**	**3rd Range**
1st Range CMD Signal	HIGH	LOW	LOW
2nd Range CMD Signal	LOW	HIGH	LOW
3rd Range CMD Signal	HIGH	HIGH	LOW

Table 1: Range Command Signals

Table 2 summarizes the output or actuated pressure-operational range logic relationship. HIGH in this case is when the sensed hydraulic pressure is greater than a predetermined threshold value (ie. greater than 0 psi). As shown, range pressure #1 signal is HIGH and range pressure #2 and #3 signals are LOW when operational range #1 is actuated. Range pressure #2 and #3 signals are similar to range pressure #1 signal. Note that the logic governing the output signals is not negated.

	1st Range	2nd Range	3rd Range
1st Range Pressure Signal	HIGH	LOW	LOW
2nd Range Pressure Signal	LOW	HIGH	LOW
3rd Range Pressure Signal	LOW	LOW	HIGH

Table 2: Range Command Signals

RANGE SOLENOID FAILURE DETECTION APPROACH

Detecting solenoid faults using this input verse output signal comparison requires pre-processing signal conditioning, or filtering. Figure 1 outlines the procedure. First the raw command signal data is low-pass filtered with an approximate 10 Hz cut-off frequency in order to remove signal noise. The resulting signals are converted to Boolean logic states (ON/OFF). Second, the raw pressure signals are similarly filtered. Once the signals are filtered the algorithm compares the signals' relative values according to the logic tables referenced above. The algorithm continually monitors the signals and discrepancies are reported as range faults.

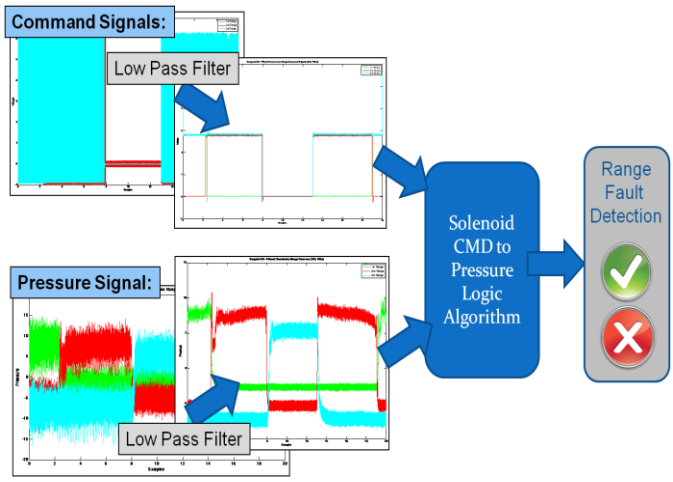

Figure 1: Solenoid fault detection processing flowchart

Transmission range shift changes are transient events. Damping and capacitive dynamics of hydraulic-mechanical systems give rise to response delays which are reflected in the system's time constant(s). Accounting for the pressure response delay in the algorithm is necessary in order to prevent false positive reporting of solenoid fault conditions.

Figure 2 illustrates the pressure response delay to a 2nd to 3rd range command signal. Note the approximate 0.35 second time lag between the point when the operational range (blue line) is commanded to 3rd range and the time required for both the 2nd range pressure signal to decrease relative to the increasing 3rd range pressure signal. The algorithm addresses this characteristic response delay between ranges by waiting 0.35 seconds after a shift command event prior to comparing signals to detect fault conditions.

For graphic designation purposes, the algorithm denotes the operational range to be '-1' during the brief instance the solenoid signals change states. It is also noted that while the response delays due to sensor dynamics contribute to the overall system delay, they are insignificant relative to the magnitude of the hydraulic-mechanical response delay.

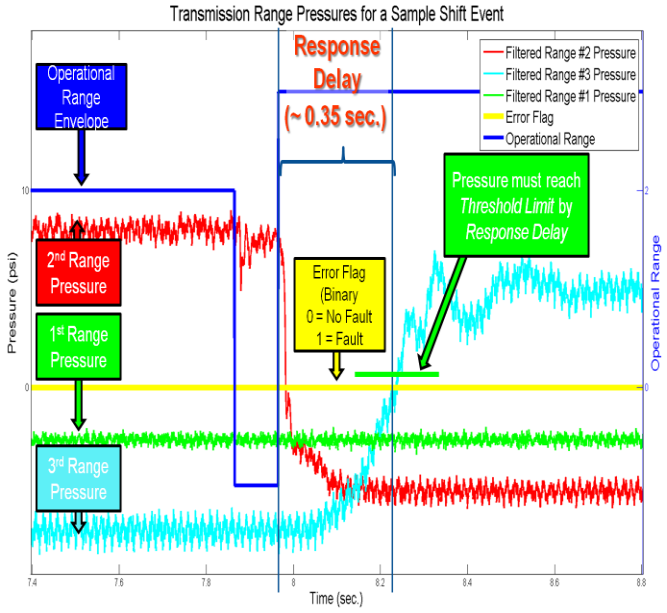

Figure 2: Range pressure signals during a shift from 2nd to 3rd range

Figure 3 illustrates series of 1st-3rd range shift events performed over a 20 sec period. This figure shows the relationship between commanded operational levels (blue line – right axis) and their respective relative hi/low pressure signal levels (green, red, cyan lines – left axis) tabulated in Table 2.

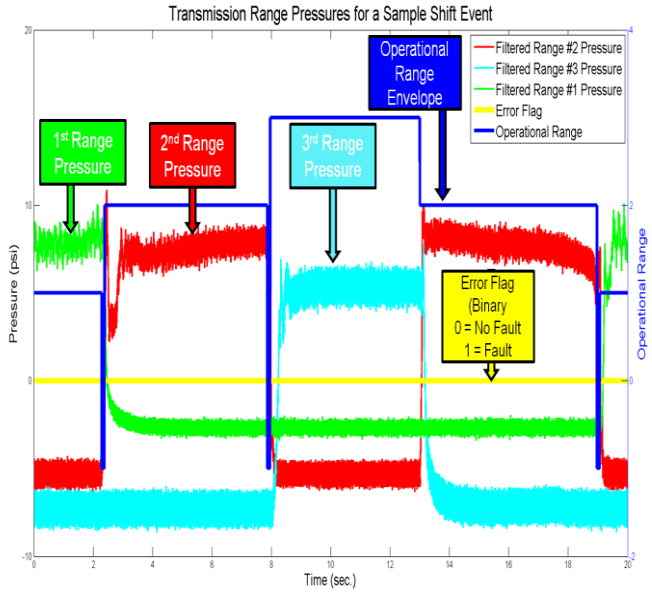

Figure 3: Range pressure signal over different shift events

TRANSMISSION #1 FAILURE DESCRIPTION

The data acquisition hardware was installed approximately half-way through the testing of transmission #1. The reliability test set-points defined by the OEM provided consistent, repeatable operating conditions at which the operational characteristics and vibratory signatures of the transmission could be compared throughout the testing. These set-points are illustrated in Figure 4, according to their output horsepower and output RPM. Vibration data was analyzed separately for each individual set-point, and data that was recorded during transient conditions (speed, load, or range changes) was discarded. This approach allowed speed and load related effects to be distinguished from damage induced changes in the measured signals. The operating speeds, loads and range of the transmission cause sufficient changes to the vibratory behavior of the system to warrant this type of analysis approach.

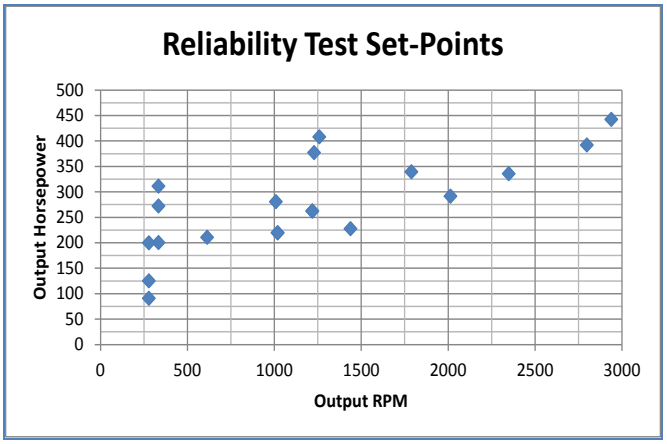

Figure 4: Steady state groups

Failure Description

This test for the first transmission was terminated when it failed to support the required load during 1st range operations. The tear-down inspection revealed a failure of the left-hand hydraulic unit. A bolt holding the actuator housing to the hydraulic unit came loose, resulting in an o-ring being blown out the front of the hydraulic unit. This resulted in obvious hydraulic pressure loss and loss of operation. In addition to the hydraulic failure, which ultimately resulted in loss of operation, the tear-down inspection revealed that the bearing supporting the 1st gear on the right-hand side had failed. Small pieces of a bearing cage had gradually been showing up in the oil sump long before the test was terminated. It was assumed that the bearing was so tightly packed that the balls were not able to

displace significantly until they had experienced significant wear. Without the cage, the transmission was able to operate for an extended period of time without exhibiting adverse effects of the damage, or any operational impairment. The tear-down inspection revealed that the raceways exhibited significant damage, and several of the balls had large areas of damage and severe wear, including flat spots. Once the balls and raceway had become significantly worn from the initial cage debris, the balls were able to displace more and more, which increased uneven load distribution, increased the amount of wear debris, and escalated damage progression. At this late stage of failure, observable indications of damage were apparent to the operators and technicians.

Analysis Results

To understand how faults in the transmission affect vibrations within the transmission, accelerometer recordings were analyzed in both the time and frequency domains for each of the test plan operating conditions. Data collected during testing was processed and analyzed applying the signal processing tools outlined above. The results of this analysis were used to identify fault indicators which could be easily integrated into an onboard health management system.

Statistical Data Analysis

Fundamental statistical processing tools were used to identify vibration fault indicator features from the data collected from transmission #1. These features included: (1) kurtosis, (2) crest factor, (3) variance, (4) root mean square, (5) skewness, (6) standard deviation, and (7) peak-to-peak amplitude. The most significant findings from these analyses are reported below.

Kurtosis

The results of the statistical analysis of the data collected during transmission #1 testing suggest that the transmission condition can be monitored by tracking the kurtosis of the vibration. Kurtosis was calculated for each data collection over every transmission operating test point group and the results indicate that this feature responds in a statistically significant manner to the developing damage, with sufficient damage sensitivity to provide in-situ detection capabilities. The processing results for transmission snapshots that were characterized by a 2,765 RPM output shaft speed and 375 ft-lbs output torque are illustrated in Figure 5.

.

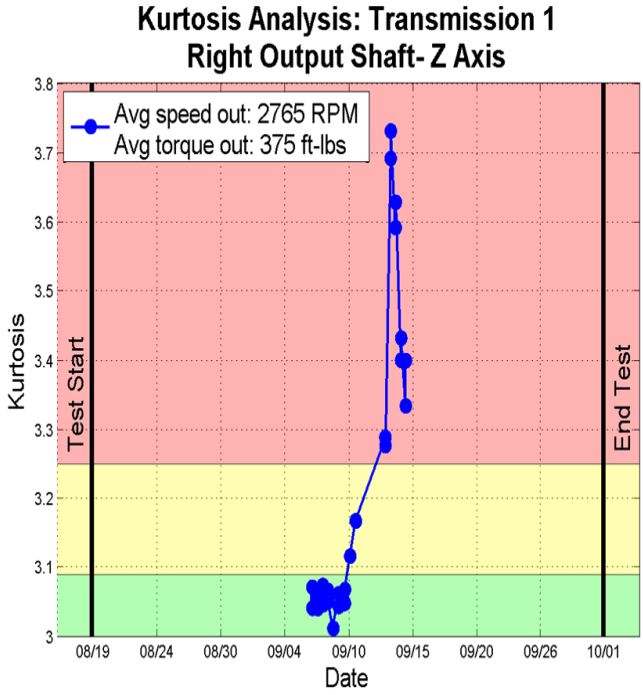

Figure 5: Transmission #1 kurtosis processing results

In the illustration in Figure 5, it is evident that the steady state groups available for analysis from the transmission #1 testing are contained in a finite time window. No steady state data at this specific speed-load set point were recorded due to the inability of the transmission to support the commanded 2,765 RPM – 375 ft-lbs set-point. The data in Figure 5 are therefore plotted on a more appropriate time scale in Figure 6 in order to more clearly capture the transition to failure that is indicated by the kurtosis feature.

An analysis of the data presented in Figure 6 reveals that the probability distribution of the vibration time history changes throughout the transmission's operating life. It is apparent that an increasing trend of kurtosis begins on September 10, and continues until the last steady state snapshot of transmission #1 testing at this set point is recorded. This rise in kurtosis indicates that there are distinct impacts being measured by the accelerometer.

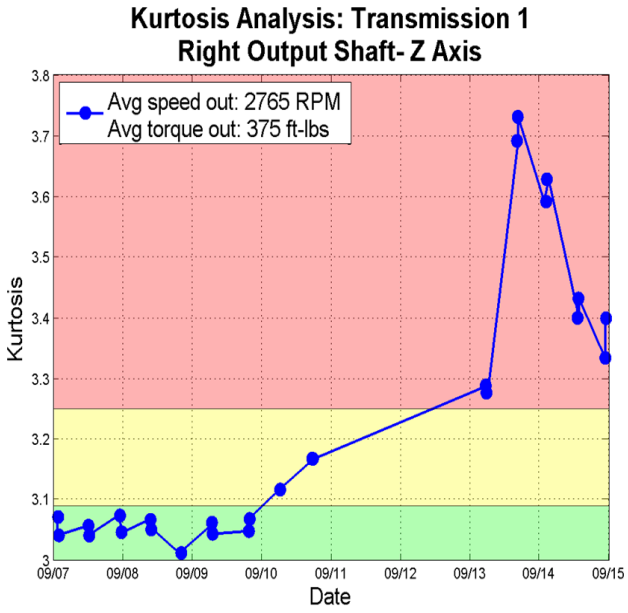

Figure 6: Detailed view of transmission #1 kurtosis processing

Physically, these irregular vibrations are likely to be caused by rolling mechanical impacts caused by gear or bearing defects, or due to the presence of wear debris circulating with the lubrication fluid that creates additional sources of impacts. As the defects grow larger, the vibration resembles a series of impulses that correlate to a statistical distribution with a lower kurtosis value than when the damage was a smaller single point-defect. Similarly, if the measured vibration is caused by wear debris, the kurtosis can decrease after the sediment is deposited in filters or sumps.

Knowing that transmission #1's primary mode of failure was a loss of functionality in the 1st gear bearing on the 3rd range side, and hydraulic failure, it is likely that this observed rise in vibration kurtosis is correlated to the these failures. Long before testing completed it was reported that pieces of bearing cage were noticed in the oil sump. The measured rise in vibration kurtosis between September 10 and September 15 is likely a direct quantifiable indication of the failing bearing cage. As pieces of the degrading bearing cage were shed into the transmission, they caused mechanical interference with other moving components of the transmission, generating vibration and inducing secondary damage, until they were deposited in the oil sump. The wear debris generated from the bearing cage typically results in distributed damage across the entire bearing, including the rolling elements and raceways.

This theory is also supported by the quality of data observed by the two accelerometer installations. While the transmission's right output instrumentation recorded a strong rise in kurtosis between September 10 and September 15, the left output instrumentation didn't observe a similar change in vibration probability distribution. This is likely to be due to the localized interference caused by the failing 1st gear right hand side bearing.

From the data presented in Figure 5 and Figure 6, it is obvious that the level of kurtosis computed from the vibration signal could be a useful tool for the predictive condition monitoring of the 1st gear bearing. The rising trend in kurtosis quantifies a degradation of the 1st gear right hand side bearing's functionality. As a result, the data presented in Figure 5 through Figure 8 are illustrated on a colored background reflecting three regions of assumed condition degradation. These regions of condition degradation are set by a kurtosis threshold. The green background signifies a fully functional 1st gear bearing, the yellow background reflects a degrading level of 1st gear bearing function, and the red signifies a critical 1st gear bearing.

Variance

An increase in the variance of the measured vibration was also observed between September 10 and September 15. The variance for the same datasets used in the kurtosis analysis is illustrated in Figure 8. Similar to the kurtosis of these datasets, the variance follows an increasing trend which starts between September 9 and September 10. It is important to note that the beginning of this increasing trend is slightly earlier than the first noticeable rise in kurtosis.

In a similar contrast to the kurtosis trend in Figure 9, the variance continues to follow this increasing trend throughout the entire dataset while the kurtosis level decreases after its peak. Physically, this indicates that the vibration amplitude began to increase soon after the 1st gear bearing cage started to fail, and continued increasing as the damage became more widespread throughout the bearing and throughout the transmission. This rise in vibration amplitude continued even after pieces of the bearing cage were filtered out of the system as a result of the higher level of vibration.

The regions of condition degradation (green, yellow, and red) are set by predetermined thresholds based on the variance data observed in these tests. The green background signifies a fully functional 1st gear bearing, the yellow background reflects a degrading level of 1st gear bearing function, and the red signifies a critical 1st gear bearing.

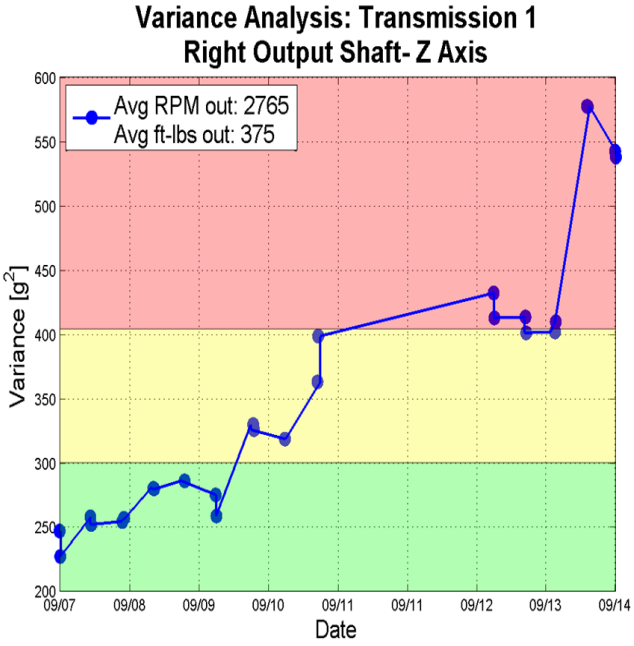

Figure 7: Transmission #1 variance statistical processing results

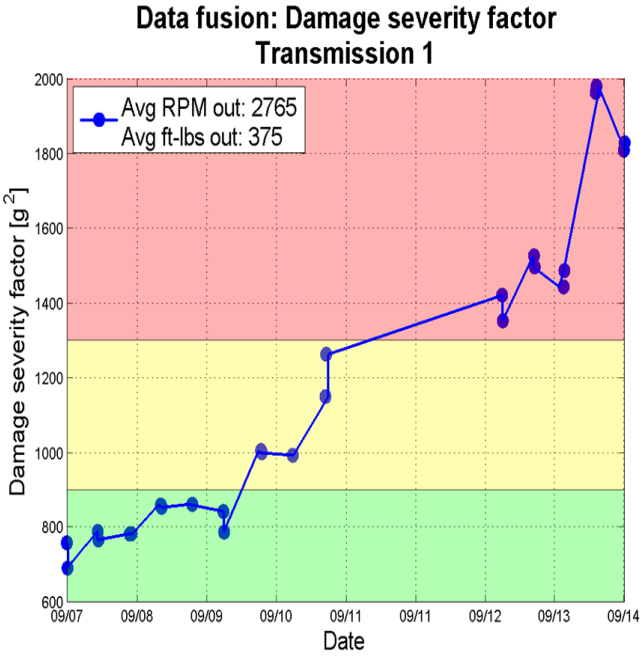

Figure 8: Transmission #1 DSF

Data Fusion – Damage Severity Factor

Data fusion is a powerful tool that could be used to create a condition monitoring feature superior to its constitutive metrics. Kurtosis is a very robust feature whose amplitude can be used to reliably monitor the condition of machinery. The problem exists, though, that for most failure mechanisms, failing machinery's vibration kurtosis often decreases after peaking. This happens when pieces of sediment which are created by component failures are filtered from the system and no longer cause irregular vibrations. If kurtosis is not calculated on a frequent enough time schedule, this peak may be wholly overlooked.

To overcome this, Kurtosis was combined with variance to create a fused feature called the Damage Severity Factor (DSF). The DSF has been calculated for the steady state set points used in previous statistical analysis and is plotted in Figure 8. Data trends suggest that the amplitude of the DSF can be used to quantify the level of damage severity for transmission #1.

DSF thresholds were set to mark three levels of damage severity for transmission #1. These three levels of operational health are signified by the green, yellow, and red background colors in Figure 8. For the illustrations in Figure 5 through Figure 8 the background colors represent a fully functional 1st gear bearing, degrading 1st gear bearing, and a critical 1st gear bearing respectively.

Transmission #1 Summary

Knowing the equations for the bearing, gear and shaft frequencies also provide a wealth of information and resolved nearly all the frequency components observed in the frequency spectrum. This is the bare essentials for even attempting to locate abnormal behavior and pin point the location of the impeding failure. While the frequency domain processing provided great insight to the operating transmission, the energy for the bearing related frequency components were very small and most likely not-measurable due to the dominating energy of the shaft and gear mesh related components in the system. One possible way to improve sensitivity to bearing related faults is optimal sensor placement. This is achieved through modal impact testing. While not performed in this effort due to time and testing schedule, this analysis should be performed before any testing commences. Modal impact testing can determine the best transmissibility between individual component and casing, thereby providing a roadmap for optimal sensor placement. This approach can also determine if a node exist in the frequency range of interest.

While the frequency domain provided a wealth of information related to the gear mesh and shaft frequencies, bearing frequency content was least apparent. However, simple time domain statistical measures provided a predictive early indication of the 1st gear bearing failure. For this transmission, kurtosis and variance were two statistical features that provided equal indications of the failure. While kurtosis is an adequate feature for indication

of the onset of failure, due to its nature it tends to decline as the failure continues to get progressively worse. Therefore, it has been shown for this transmission that fusing another feature, in this case variance, provided a superior feature. Specifically this means that we want a feature that continues to rise as the fault severity continues to worsen. The fused feature which ARL called the Damage Severity Factor (DSF) in Figure 8 demonstrates this idealistic result.

Again, the regions of condition degradation (green, yellow, and red) are set by predetermined thresholds based on the observed data in these tests. The green background signifies a fully functional 1st gear bearing, the yellow background reflects a degrading level of 1st gear bearing function, and the red signifies a critical 1st gear bearing.

TRANSMISSION #2 FAILURE DESCRIPTION

The failures experienced during the testing of transmission #2 were similar to the bearing failure during the first transmission test. The tear-down inspection revealed that the bearing supporting the 1st gear on the left-hand side had failed in a similar manner as in the previous test, where pieces of the cage were observed in the oil sump long before any indications of failure had been observed. In addition to this bearing failure, a nearby bearing supporting the 2nd range output-side sun gear and 2nd range B-average gear was also significantly damaged. The outer race of this latter bearing split in two pieces (longitudinally, so that there were two rings). Two separate sets of beach marks were clearly visible, indicating the location at which crack initiation occurred, and the direction of propagation. A 1.5" length of material was also missing from an inside edge of the raceway. In particular, the beach marks formed a 180-degree angle facing away from the center-line of the bearing. This, in addition to the fracture surfaces, indicated that the bearing appeared to fail under high axial loads. A lock-washer, riveted to the 3rd range planetary sun gear had also been damaged during the testing. The rivets were sheared off by a sharp edge of the rivet holes on the washer that created a location of stress concentration. This was not considered a significant design issue, and is probably an atypical secondary failure that developed after significant damage had already accumulated. At approximately 330 hours of testing, in December 2010, the first pieces of broken cage material were appearing in the oil sump, although it is not clear which bearing failed first, or if the one failure directly caused the second failure. The pieces of the cage that were collected were uniformly bent in half, which indicated that they had broken off and been rolled over by the balls.

All 3 of the failed bearings from tests #1 and #2 exhibited signs that severe cage damage preceded damage to the raceway and balls (this was deduced from the fact that pieces of the cage appeared prior to any observable changes in overall vibration levels, which would be associated with severe raceway and ball damage). In general, the bearing failures seemed to indicate high thrust loads resulting from the bevel gear-set (which is the first gear-set from the input shaft). This gear-set produces reactionary forces in the axial direction that are maximized under high load dynamic conditions. One possible condition where this might occur is during the shift between 2nd and 3rd range. The instantaneous change in hydraulic stroking that occurs during this shift could result in a disparity in loading between the hydraulic A-end gear-path and the mechanical gear path to the output planetary ring gears. This creates a torsional shock that is probably difficult to estimate and measure, from a design and analysis perspective. As a result, it would not be surprising if this condition was not fully designed into the requirements of the bearing load-rating capacity. However, it is not clear that this was the root cause of failure. The post test tear-down inspection revealed significant damage to the bearings, which precluded an obvious determination of the initial cause of the failure.

Analysis Results

The same statistical and spectral processing techniques used to examine data collected during transmission #1 testing were used to inspect the transmission #2 datasets. These processing techniques included: (1) kurtosis, (2) crest factor, (3) variance, (4) root mean square, (5) skewness, (6) dataset standard deviation, and (7) peak to peak amplitude. The most significant findings from these analyses are reported below.

Statistical Data Analysis

Prior to statistical processing, steady state set point groups were compiled for each of the test plan set points. These groups were used to examine statistical features of the vibration time history for the transmission #2 testing at similar transmission operating conditions.

Kurtosis

Kurtosis was calculated for each of the steady state set point groups and graphically examined. Figure 9 illustrates the kurtosis trend for the 2340 RPM, 375 ft-lb group throughout transmission #2 testing.

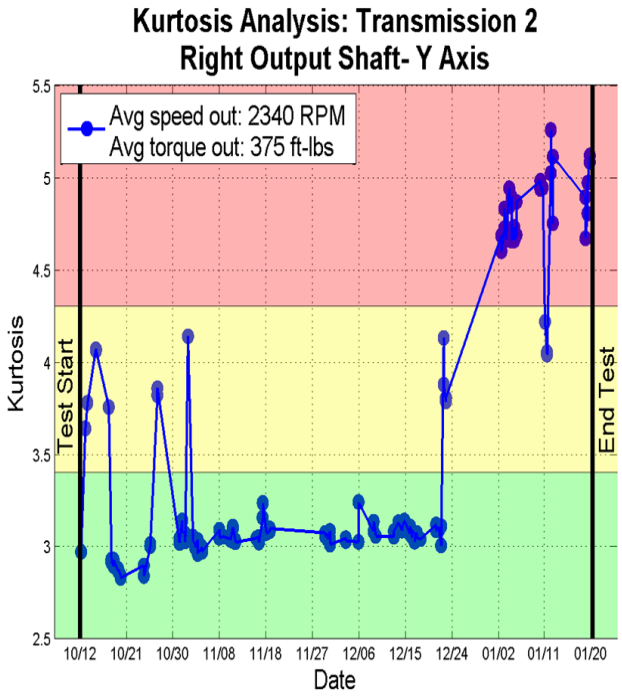

Figure 9: Transmission #2 kurtosis processing results

The data illustrated in Figure 9 shows three peaks of elevated kurtosis values following the start of transmission #2 testing. These events occur between October 12 and November 4. After these events, there is a consistently low period between November 4 and December 23. Following this low period, kurtosis again rises and remains high until the end of testing.

When assembling complex machinery it is usually difficult to get perfectly manufactured and installed components. The break-in period after machinery is newly assembled generates component wear that typifies gear vibration, so it is not a surprise to see some initial response of the kurtosis. It is also possible that the elevated responses observed at the early part of the test were due to incipient damage that briefly manifested changes in the dynamic behavior of the transmission, without causing significant permanent damage. To gain insight into the possible cause of the rises in vibration kurtosis between October 12 and November 4, raw vibration time histories were examined and transmission test logs were reviewed. Neither the raw data nor maintenance test logs provided information confirming particular component failures in the transmission during this time period. Although the specific cause of these rises are unknown, it is possible that the first three events evident in Figure 9 are associated with the transmission's break in operation.

The consistent kurtosis levels near 3.0 between November 4 and December 23 reflect nearly 12 weeks of normal transmission operation. After December 23, a steep rise in the magnitude of vibration kurtosis is visible in Figure 9. This rise in value is likely due to deterioration in the functional capability of the transmission. Unlike the kurtosis trends recorded near the ultimate failure of transmission #1, the magnitude of kurtosis observed near the completion of transmission #2 testing remained consistently high. This difference demonstrates the variability in the failure process, and the challenge of interpreting individual condition indicators. Although a failure in the 1st gear bearing led to ultimate failure in both transmissions, it's possible that not all pieces of the deteriorating bearing cage were captured in the oil sump. In this scenario, vibration kurtosis would remain high instead of peaking as in transmission #1 experiments.

A comparison of Figure 6 and Figure 9 show that the peak kurtosis levels for transmission #2 is 23% larger than those recorded from transmission #1. This is because the vibration probability distribution function is dependent on the vibration mechanics individual to each transmission build. As a result, kurtosis thresholds will also be individual to each transmission. Figure 9 is plotted with the same three color bands used in Figure 6. These bands represent thresholds placed on vibration kurtosis that can be used to characterize the condition of transmission #2's operation throughout the second test. As in previous figures, a green background signifies a fully functional 1st gear bearing, a yellow background reflects a period of degrading level of 1st gear bearing function, and the red threshold signifies a critical 1st gear bearing.

Transmission #2 Summary

Much like the result found for transmission #1, the frequency domain provided a wealth of information for the gear and shaft related frequency components. However, the bearing frequencies again were least apparent. Like transmission #1, the simple time domain statistical measures provided a means of an early indication of failure. For this transmission, kurtosis alone provided an adequate means of measure for failure. While not shown here, other statistical metrics could be fused to further enhance the feature performance. The Damage Severity Factor in this case would simply be kurtosis which is presented in Figure 8.

CONCLUSION

The bearing failures experienced during testing of transmissions 1 and 2 presented obvious similarities, and there are several conclusions that can be drawn from the results. The severe deterioration of the bearings that occurred prior to any obvious impact to the functional operation of the transmission clearly indicated that the gears are conservatively designed, allowing them to absorb significant abuse with little consequence. The OEM confirmed that gear failures seldom occur in the field. As a result, there is little need to develop algorithms specific to gear-related failure modes. Additionally, the bearing failures that were experienced in tests 1 and 2 were not characteristic of the types of failures that are generally observed in the field. This could have resulted from the re-use of worn components in build assembly of these test transmissions, or certain aspects of the test-cell environment or test plan, etc. In particular, the OEM indicated that hydraulic system failures represented the most common mechanical failure types, whereas the existing EA is generally regarded as having the most reliability issues on the existing transmission. For this effort, simple statistical analysis and data fusion techniques provided a simple baseline for developing a lightweight, embedded diagnostic/prognostic module for ground vehicles.

REFERENCES

[1] Zakrajsek, James J., NASA Technical Memorandum 102340, Lewis Research Center, Cleveland, Ohio,

[2] Mitchell Lebold, Katherine McClintic, el.al, "Review of Vibration Analysis Methods For Gearbox Diagnostics and Prognostics", 54th Meeting of the MFPT, Virginia, May 2000

[3] Moubray, J., Reliability-centered Maintenance, 2nd ed., Industrial Press, Inc., NY, 1992

BIBLIOGRAPHY

Mitchell Lebold is a Research Engineer with the Applied Research Laboratory at The Pennsylvania State University with more than fifteen years of experience in algorithm development and embedded monitoring systems. He holds an M.S. and B.S. degree in Electrical Engineering from Pennsylvania State University. Mr. Lebold leads several multi-disciplinary research and development projects in the areas of wireless smart sensors, algorithm development, and open standards for condition-based maintenance. He has designed and developed numerous custom test and measurement systems as well as embedded wireless data acquisition systems for machinery health monitoring. His current research involves engine and driveline diagnostics and prognostics algorithm development

Scott Pflumm is a research engineer at the Applied Research Laboratory. He received his B.S.M.E and M.S.M.E in Mechanical Engineering from Penn State University in 2002 and 2005 respectively. His current work at ARL is in support of test and analysis of failure modes for ground vehicles at the sub-system and component level.

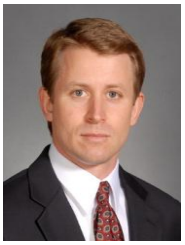

Jason Hines is an Associate Research Engineer with the Applied Research Laboratory at the Pennsylvania State University with 10 years of experience in fault diagnostics and prognostics development for a variety of electro-mechanical systems. His research focus is the development of advanced signal processing algorithms for enabling prognostic reasoning capabilities within practical real-world operating scenarios. He has a B.S. and M.S. in Mechanical Engineering from The Pennsylvania State University. His research activities have involved aerospace systems (AH-64D, SH-60B, CH-46E, F-35 STOVL), and ground systems (M1A2, M2 and M3 BFV, Stryker, Medium Tactical Vehicle Replacement). His current research focus involves the development and implementation of particle filtering techniques for nonlinear Bayesian forecasting of diagnostic indicators.

Jeffrey Banks is the Department Head of Complex Systems Engineering & Monitoring and he has 17+ years experience in applying advanced signal processing techniques, intelligent systems technology, and embedded diagnostics / prognostics tools to condition monitoring applications for the US Navy, US Marine Corps, US Army, NASA and Industry. His education includes a B.S.M.E. from Villanova University and a M.S. in Acoustics from The Pennsylvania State University.

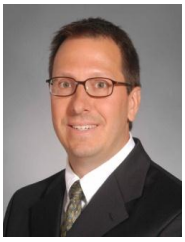

His research engineer duties include developing machinery health management systems and diagnostic and prognostic technology for various DoD assets including the U.S. Marine Corps Expeditionary Fighting Vehicle (EFV), Light Armored Vehicle (LAV), AV-8B Harrier, U.S. Army Heavy Expanded Mobility Tactical Truck (HEMTT), and Heavy Brigade Combat Team M1A2 Abrams, M2/M3

Bradley Fighting Vehicle, M88 Hercules platforms. He has developed two short courses at all NASA facilities in the areas of Condition Based Maintenance (CBM) and Reliability Centered Maintenance (RCM). Additional responsibilities include conducting degrader analyses for a variety of complex systems and platforms including aircraft engines and combat ground vehicles. He has also designed and developed diagnostic instrumentation systems for machinery failure test beds and field data acquisition systems. Mr. Banks has first authored and published more than 50 conference papers and technical reports.

Jonathan Bednar is a Graduate Research Assistant with the Applied Research Laboratory at The Pennsylvania State University. He earned his B.S. degree in Mechanical Engineering in 2010 from The Pennsylvania State University and will complete his M.S. degree in 2012 focusing in acoustics and vibrations. His current research includes condition monitoring of Compression Ignition engine crankshafts using torsional features and the optimization of a high-temperature pressure sensing device.

Disclaimer: Reference herein to any specific commercial company, product, process, or service by trademark, manufacturer, or otherwise, does not necessarily constitute or imply its endorsement, recommendation, or favoring by the United States Government or the Department of the Army (DoA). The opinions of the authors expressed herein do not necessarily state or reflect those of the United States Government or the DoA, and shall not be used for advertising or product endorsement purposes.